Earth, Planets and Space

FULL PAPER Open Access

Investigation of the subsurface structure at the target site in Kumamoto, Japan, and the distributed data of the blind prediction exercise: report for the experiments for the 6th international symposium on effects of surface geology on seismic motion

Shinichi Matsushima[1*], Hiroaki Yamanaka[2], Seiji Tsuno[3], Kosuke Chimoto[4], Haruhiko Suzuki[5], Hiroshi Kawase[1] and Takeshi Matsushima[6]

Abstract

This technical report explains details on the results of the investigation to build a subsurface structural model and a selection of earthquake data at the target site of the blind prediction exercise for "The 6th International Association of Seismology and Physics of the Earth's Interior/International Association of Earthquake Engineering International Symposium on the Effect of Surface Geology on Seismic Motion (ESG6)." The selection process of the target site in the Kumamoto Plain, Japan, in ESG6 was explained with a historical review of the blind prediction tests in the previous ESG conferences. We have collected existing subsurface structural and earthquake data and conducted geophysical and geotechnical surveys in and around the target site to generate important velocity structure and the earthquake data used in the blind test. Microtremor data were obtained in triangular arrays ranging in side lengths from 1 to 962 m, and active surface wave data were derived along a 36-m line at the site. These data were provided for the prediction of a subsurface structural model in the first step of the blind prediction exercise. We also conducted a velocity logging in a borehole to a bottom depth of 39 m at the site and laboratory tests of soil samples from the borehole. We constructed a velocity profile of the shallow and deep sedimentary layers from a combination of the geophysical and geotechnical data at the site, and validated it by comparing the characteristics of the ground motion data from the moderate event. This "preferred velocity model" was provided as a standard model to the participants in the second and third steps of the blind prediction test to predict the earthquake ground motions of a moderate event and the mainshock of the 2016 Kumamoto earthquake.

Keywords ESG6, Blind prediction, 2016 Kumamoto earthquake, Kumamoto City, Microtremor, Ground motion, P-S logging, In situ measurement

*Correspondence:
Shinichi Matsushima
matsushima.shinichi.6r@kyoto-u.ac.jp
Full list of author information is available at the end of the article

Graphical Abstract

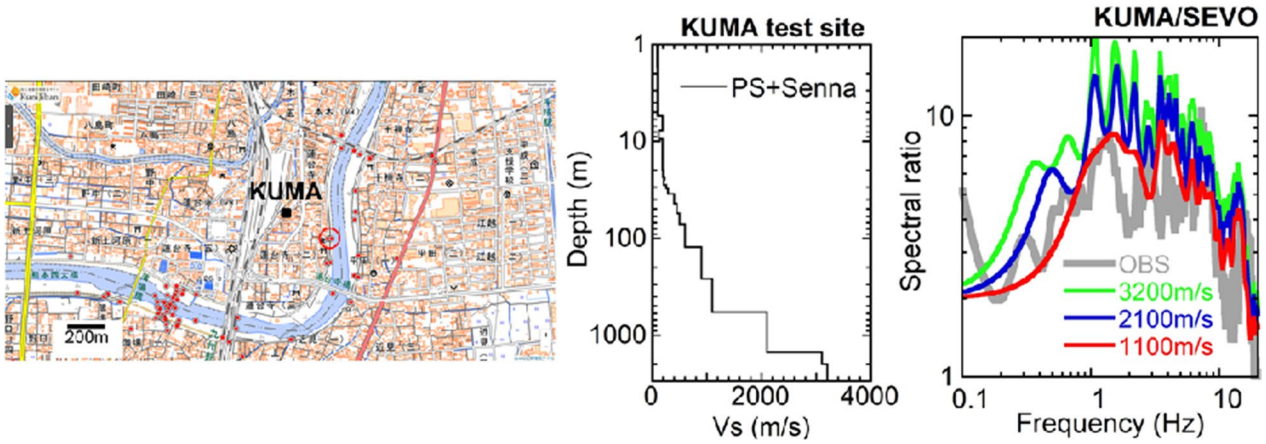

Introduction

Introduction of JWG-ESG

In 1985, the resolution for the General Assembly of the International Association of Seismology and Physics of the Earth's Interior (IASPEI) included a proposal by Dr. Brain E. Tucker, then Acting State Geologist of California, to "propose to the International Association of Earthquake Engineering (IAEE) the formulation of a joint working group to promote studies on the Effects of Surface Geology on Seismic Motion (ESG)." The following year, Dr. Tucker contacted Prof. Kazuyoshi Kudo, then Assistant Professor at the Earthquake Research Institute, University of Tokyo (ERI), to approach IAEE. Prof. Kudo contacted Prof. Yutaka Osawa, Professor at ERI and then Secretary General of IAEE. Prof. Osawa contacted Prof. Wilfred D. Iwan, then a professor at the California Institute of Technology, to represent IAEE, and Prof. Iwan agreed. Thus the framework for the joint working group between IASPEI and IAEE was established. The establishment of the IASPEI/IAEE Joint Working Group on Effects of Surface Geology on Seismic Motion (JWG-ESG) was proposed by the co-chairs, Dr. Tucker and Prof. Iwan. In response to the JWG-ESG in Japan, the Earthquake Engineering Sub-Committee was established as an advisory body to the Earthquake Engineering Liaison Committee of the Science Council of Japan (Kudo 2021).

The first ESG workshop by JWG-ESG was held during the General Assembly of IUGG in Vancouver, Canada in 1987. During the first ESG workshop, a resolution was adopted that included the establishment of JWG-ESG, the establishment of the steering committee, the consideration of Turkey Flat, California and Ashigara Valley, Japan, as test sites, and the holding of the second ESG workshop in Tokyo in 1988 as the 9th World Conference on Earthquake Engineering (9WCEE) was to be held in Tokyo (CDMG, 1998). During the second ESG workshop, the steering committee summarized the requirements for an international test site and officially assigned Turkey Flat as the first test site for ESG. Ashigara Valley was assigned by the steering committee during the IASPEI conference held in Istanbul, Turkey, in 1989.

In 2003, JWG-ESG had to be reconstituted due to the change of IASPEI commission. Prof. Hiroshi Kawase, then a professor at Kyushu University, became the co-chairman for the IASPEI side and Prof. Jacobo Bielak, then a professor at Carnegie Mellon University, became the co-chairman for the IAEE side. The members of the steering committee was also reformed and approved during the IASPEI meeting in 2003. As of September 2022, the co-chairs are Prof. Kawase and Prof. Jamison Steidl, Adjunct Professor at the University of California, Santa Barbara.

History of ESG symposia and past blind predictions

The first international symposium on ESG (hereafter ESG1) was held on March 25–27, 1992 at the City Hall of Odawara City, Japan, which is located near one of the two test sites, Ashigara Valley (JWG-ESG 1992). The main topic of ESG1 was to discuss the blind prediction results of weak motion observed at Turkey Flat and both weak and strong motions observed at Ashigara Valley. The blind prediction exercises were performed prior to ESG1 and the results were reported at the symposium. The summary of the Ashigara Valley blind prediction exercise can be found in Kudo (1992) and Kudo and Sawada

(1992) for the distributed and blind data and Midorikawa (1992) for the presented results. In essence, considering the inherent variations for multiple observations at the same site, which are now known to be less than half or twice the average, their overall agreement with observations was statistically satisfactory. We also found that the variability between predictions was reasonably small, since it is also less than the inherent variations for multiple observations. We should mention that there were a few participants whose results were exceptionally larger or smaller than the others. This fact strongly suggests the need to screen the participants before the blind prediction.

The second international symposium on ESG (hereafter ESG2) was held at the Research and Development Center of the then Tokyo Electric Power Company in Yokohama, Japan from December 1 to 3, 1998. The main feature of ESG2, was the Simultaneous Simulation (hereafter SS) for Kobe earthquake that occurred on January 17, 1995. The SS was an open prediction competition, and its purpose was threefold: (1) to compare the simulated synthetics submitted by participants from around the world; (2) to understand the key parameters for quantitative prediction of strong ground motions; and (3) to explore future research directions related to the ESG study and strong motion prediction through the results of the SS. Iwata et al. (1999) summarized the experimental settings and data provided, while Kawase and Iwata (1999) summarized the results submitted. The results presented were more or less satisfactory, and the necessity of the 3D basin structure for the quantitative prediction of the observed strong motions in Kobe was confirmed. The most interesting finding was the fact that that the variation between the simulations of different parties was considerably smaller when the observed data were provided, but much larger when no observed data were provided. The general chairman for both ESG1 and ESG2 was Prof. Hiroshi Okada, then a professor at Hokkaido University.

The third international symposium on ESG (hereafter ESG3) was held in Grenoble, France from August 30 to September 1, 2006. It was chaired by Dr. Pierre-Yves Bard, then a senior researcher at LGIT. Two blind prediction exercises were performed for ESG3. The first was to estimate the phase velocity from the provided microtremor data, which were simulated microtremors by synthetics and observed microtremors by array observations in the Grenoble basin (Cornou et al. 2009). Second, the simultaneous simulation of the 3-D basin response of the Grenoble basin was performed (Chaljub et al. 2009). As for the microtremor blind experiment, they reported quite convincing evidence for the effectiveness of the array microtremor method, with several caveats. Regarding the simultaneous simulation of the 3D basin response, they found that the matching between the synthetics of different participants was not as good as expected. Later, they found that the discrepancy between participants was mainly caused by various human factors. This is a similar problem to the open prediction experiment during ESG1 mentioned above.

The fourth international symposium on ESG (hereafter ESG4) was held at the University of California Santa Barbara (UCSB) from August 23 to 26, 2011. Prof. Ralf Archuleta, then a professor at UCSB was the General Chairman. The main topic of ESG4 was to discuss the validity of Vs30, the time-averaged S-wave velocity of the top 30 m of the subsurface.

The fifth international symposium on ESG (hereafter ESG5) was held in Taipei, Taiwan, from August 15 to 17, 2016. The General Chairman was Prof. Kuo-Lian Weng, then professor at the National Central University. The main theme of the symposium was "Challenges of Applying Ground Motion Simulation to Earthquake Engineering."

Introduction of ESG6

The sixth international symposium on ESG (hereafter ESG6) was originally planned to be held in Kyoto, Japan, in March 2021 to commemorate the quarter century since the 1995 Kobe earthquake and the decade since the 2011 off the Pacific coast of Tohoku earthquake. Unfortunately, due to the difficult conditions caused by the COVID-19 pandemic, ESG6 was postponed and was held from August 30 to September 1, 2021.

After the first two ESG symposia were held in Japan, three ESG symposia were held in France, USA and Taiwan over the period of 20 years. The Japanese working committee proposed and was approved to hold the ESG symposium in Japan at the JWG-ESG steering committee held during ESG5. The local organizing committee for ESG6 was formed within the Japan Association for Earthquake Engineering (hereafter JAEE). The main theme of ESG6 was decided as "Progress of ESG research during the last three decades—How accurately can we predict site amplification?"

There were two main features in ESG6. First is the blind prediction exercise to post-predict the ground motion and subsurface structure in Kumamoto, Japan. Second is the special session on the use of data from Kyoshin Network (K-NET) and Kiban Kyoshin Network (KiK-net) operated by the National Research Institute for Earth Science and Disaster Resilience (hereafter NIED). The General Chairman was Prof. Kawase, Program-Specific Professor at the Disaster Prevention Research Institute, Kyoto University.

In order to investigate the subsurface structure of the target site of the blind prediction exercise, a thorough

investigation including several types of surveys was conducted in and around the target site. This article describes the blind prediction exercise and the data obtained from the surveys.

Blind prediction exercise

Overview

The blind prediction exercise (hereafter BP) for ESG6 was designed to post-predict a target recorded waveform, an undisclosed strong ground motion record during the 2016 Kumamoto earthquake at a site in Kumamoto City, Kumamoto, Japan (hereafter KUMA), using ground motion records from moderate-sized earthquakes, ground motion records at a reference rock site and information about the subsurface velocity structure at the site. The prediction results submitted by the BP participants were to be complied and compared with the target strong ground motion record in order to discuss about the accuracy of ground motion prediction methods and their reliability, and to understand the current status of ground motion prediction technique as a community in order to reveal the direction of development of ground motion prediction methods. The BP of ESG6 consists of three steps, Step (1) Estimation of the subsurface velocity structure (hereafter BP1), Step (2) Post-prediction of weak ground motion (hereafter BP2), and Step (3) Post-prediction of strong ground motion (hereafter BP3). The BPs are also intended to show how the accuracy of BP1 and BP2 leads to the accuracy of BP3.

Selection of the test site

The location of the target test site for the BP of ESG6, KUMA is a strong motion observation site located in Kumamoto City, Kumamoto, Japan in the northern part of the Kumamoto Plain. Figure 1 shows the location of Kumamoto City and Fig. 2 shows the detailed location of KUMA in Kumamoto City. The characteristics of the strong ground motion during the 2016 Kumamoto earthquake near JR Kumamoto Station, which is about 1 km north of KUMA, were investigated by Tsuno et al.

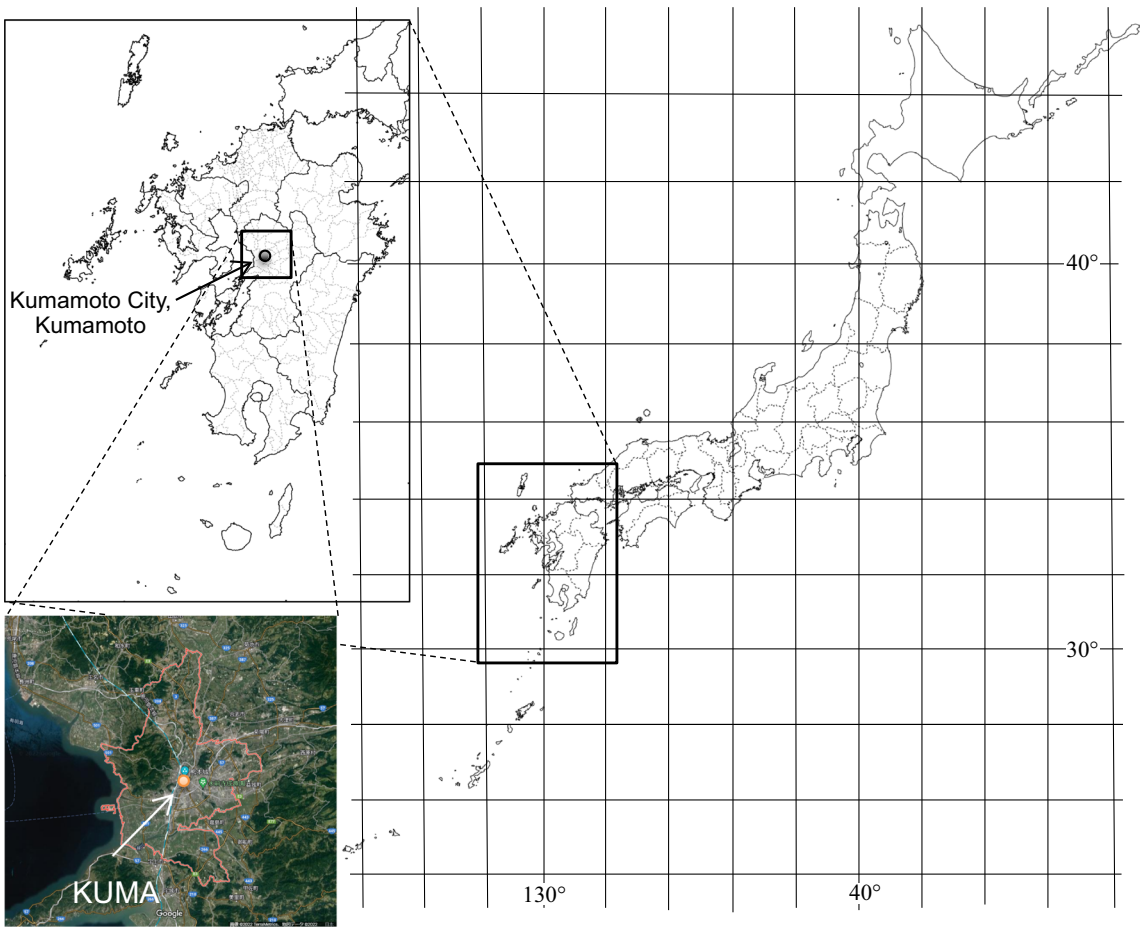

Fig. 1 Location of the target test site, KUMA, for the blind prediction exercise of ESG6, Kumamoto City, Kumamoto, Japan. The lower left map is plotted on Google Map

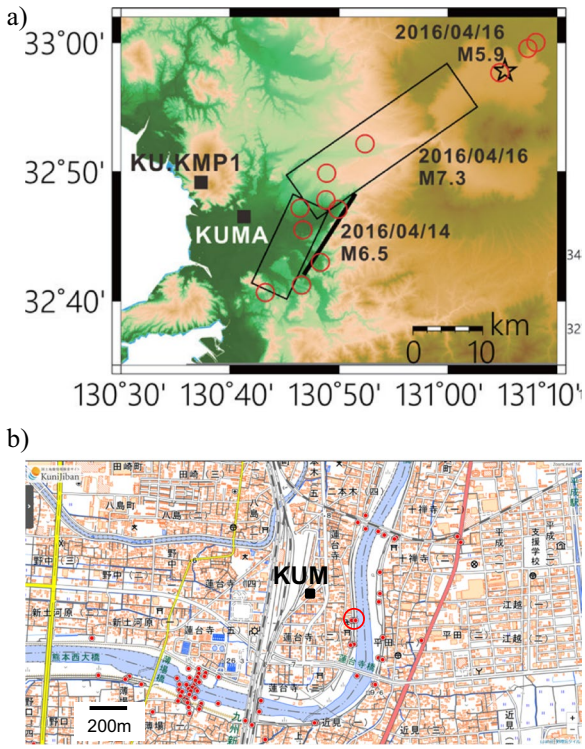

Fig. 2 **a** Map showing the location of the target test site KUMA and the reference rock site KU.KMP1 in Kumamoto City, Kumamoto, Japan, along with the locations of strong ground motion stations and epicenters of earthquakes provided in the blind predictions (BP2 and BP3). Circles indicate the epicenters of aftershocks of the 2016 Kumamoto earthquake sequence. A black star indicates the epicenter of another aftershock, which is the target earthquake in BP2. Source fault planes of the foreshock (straight line) and the mainshock (two rectangles) of the 2016 Kumamoto earthquake sequence by Asano and Iwata (2016) are projected, which are the target earthquakes in BP3. **b** Map of the detailed location of KUMA on the right bank of the Shirakawa River, plotted on Kuni-jiban (2022). Borehole survey data in Kuni-jiban for location indicated by the red circle are used as reference for the results of SPT at the borehole survey near KUMA

(2017), but the ground motion records at the target test site were not disclosed until ESG6 was held in August 2021. A preliminary microtremor observation was conducted at KUMA to check whether there was strong lateral heterogeneity in and around the site, and it was found that there was no strong lateral heterogeneity.

The condition of the strong observation site KUMA is shown in Additional file 1: Figure S1a in the electronic supplementary material. The accelerometer at KUMA was installed in a surface observation case right next to a three-story reinforced concrete building, as shown in Additional file 1: Figure S2. For the blind prediction exercises during the previous ESG symposia, ground motion records of nearby reference rock site were provided to estimate the ground motion on the sediment. For the BP of ESG6, the ground motion records were provided at a nearby rock site KU.KMP1 shown in Additional file 1: Figure S1b. KU.KMP1 is located on Mt. Kimbo north-west of KUMA as shown in Fig. 2a, which is operated by the Institute of Seismology and Volcanology, Kyushu University. Velocity meters are installed in the observation hut and the observed data were distributed to the participants of BP2 and BP3.

Three steps of the exercise

Step 1

The exercise of BP1 was to estimate a one-dimensional (1-D) subsurface S-wave velocity structure beneath KUMA, which will be used to evaluate the site amplification characteristics of the subsurface structure. The site amplification factors are necessary to predict the ground motions at KUMA. The information and data distributed to the participants were collected at the site by the members of the ESG research committee of JAEE and the General Proposal Type Research of the Core-to-Core Collaborative Research between Earthquake Research Institute, The University of Tokyo and Disaster Prevention Research Institute, Kyoto University (Chimoto et al 2020). The distributed data include microtremor data from several equilateral triangular arrays of sides lengths ranging from 1 to 962 m and surface wave data from active source measurements, which will be presented in the "Data acquisition" section. Participants were asked to analyze the vertical component of the microtremor data from the arrays and/or the surface waves from the active source measurement for Multi-channel Analysis of Surface Waves (MASW) to obtain and submit a Rayleigh wave dispersion curve using any algorithm(s). A 1-D velocity model estimated from the Rayleigh wave dispersion curve was also requested. There was also an option to submit an additional dispersion curve and 1-D velocity model using the horizontal component(s) of microtremors. Upon submission, a description of the analysis procedure was requested along with the data of the results of the analysis.

The results of BP1 are reported by Chimoto et al. (2023).

Steps 2 and 3

The exercise of BP2 and BP3 were simulations of weak motion and strong motion observed at the KUMA, which are the foreshock and mainshock of the 2016 Kumamoto earthquake, respectively. A dozen earthquake records observed at the test site and the reference site were made available to the participants, which are presented in the "Data acquisition" section. The earthquake records observed at KUMA for the target earthquakes (foreshock and mainshock) were blindfolded. The earthquake

ground motions for the target earthquake at KUMA were requested from the participants. The calculations should be based on any simulation technique such as 1-D method, Ground Motion Prediction Equations (GMPEs), empirical Green's function method, or the two-dimensional (2-D)/three-dimensional (3-D) simulations. For submission, the minimum requirement was acceleration motions for a horizontal component with a sampling frequency of 100 Hz and the Fourier spectrum in the reliable frequency range, describing the start time of the recording and the duration in the simulation. Submission of two or three component data was optional but preferred. Any other relevant information about the parameters used in the simulation was also required. For theoretical methods, a description of the subsurface velocity model used was requested. If submitted, a description of the analysis procedure was requested along with the data of the results of the analysis.

The results of BP2 and BP3 are reported by Tsuno et al. (2023).

Site information

Overview

The borehole survey was conducted at the premises of an affiliate of Kyushu Railway Company (JR Kyushu) which is located south of JR Kumamoto station in Kumamoto City, Kumamoto, Japan, as shown in Figs. 1 and 2. The borehole survey site was located approximately 30 m north-west of KUMA. The borehole survey was conducted between November 1 and 23, 2019, and the laboratory tests were conducted by OYO Corporation between December 4 and 23, 2019. The information of the results presented in this paper is based on the report by OYO Corporation. The latitude and longitude of the borehole survey site is 32.7758 N and 130.6878 E, respectively, based on the report.

The borehole survey site is located on the right bank of Shirakawa River, which flows north–south in Kumamoto City. It is located on the flood plain of the Shirakawa River and the elevation is 9 m. The surface geology of the site is alluvium that forms the flood plain of the Shirakawa River and is covered with modern landfill. The Mt. Mannichiyama, which is located north-west of the site, is formed by the volcanic rock (tuff breccia) of Mt. Kimbo. The Takuma Plateau on the eastern side of Kumamoto Plain is formed by a layer of pumice derived from the pyroclastic flow deposits of Mt. Aso and covered by a few meters of gravelly sand.

The subsurface structure at the survey site consists of landfill at the surface, Holocene sand/silt to a depth of 30 m, and then about 10 m of gravel sand layer. Below this layer is the pumice layer of Mt. Aso origin and the tuff breccia of Mt. Kimbo exists. The tuff breccia layer is considered to be the engineering bedrock at this site.

Borehole survey

A borehole survey was conducted at a point approximately 30 m north-west of KUMA. The depth of the borehole was 39 m. For the in situ measurements, the Standard Penetration Test (SPT) was conducted for every 1 m, for a total of 38 times. Undisturbed samples for laboratory testing were obtained by thin-walled tube sampling for three samples at the depths of 4 to 5 m (T-1), 7.65 to 8.65 m (T-2), 23 to 23.72 m (T-5), and rotary triple-tube sampling for two samples at depths of 13 to 14 m (Tr-3) and 20 to 21 m (Tr-4). The borehole log with N-values obtained from SPT and detailed depth locations of the samples are shown in Fig. 3.

Result of SPT at a location approximately 300 m south-east of the borehole survey site, shown as a red circle in Fig. 2, that can be found in Kuni-jiban (2022) is shown in Fig. 4. It shows that the upper 23 m is mostly sandy layers with N-values of about 20 or less, except between the depth of 18 and 21 m where N-value exceeds 30. The N-value becomes small again at about 23 m depth, where there is a silt layer with a thickness of about 3 m. The sandy layer reappears up to the depth of 35.5 m where the gravel layer appears and the N-value reaches 50. These characteristics are similar to those shown in Fig. 3.

P-S logging

P-S logging by suspension method was conducted for every 0.5 m in depth, for the entire 39 m. The result of P-S logging with boring log is shown in Fig. 5. The soil conditions and velocity profile obtained by the P-S logging are shown in Tables 1 and 2, respectively. The P-wave and S-wave waveforms are shown in Additional file 1: Figures S3 and S4, respectively, in the electronic supplement.

Laboratory tests

Laboratory tests were performed on the five samples obtained at the site. The laboratory tests were performed based on the Japanese Industrial Standard (JIS) and the Japanese Geotechnical Society Standard as shown in Additional file 1: Table S1 in the electronic supplementary material. The results of the laboratory tests for the five samples, T-1, T-2, Tr-3, Tr-4 and T-5, are summarized in Additional file 1: Table S2. The particle size distributions for each sample are shown in Additional file 1: Table S3. Specimen conditions and test results of the cyclic triaxial test to determine the deformation properties of geomaterials are shown in Table 3. Additional file 1: Tables S4 to S8 show the Young's modulus—strain (E-ε_a), hysteric damping—strain

(h-ε_a) relationships of samples, T-1 T-2, Tr-3, Tr-4 and T-5, respectively, and Additional file 1: Tables S9 to S13 show the shear modulus—shear strain (G-γ), hysteric damping—shear strain (h-γ) relationship of samples. Figures 6 and 7 show the figures of the E-ε_a, h-ε_a relationships and G-γ, h-γ relationships of specimens T-1, T-2, Tr-3, Tr-4 and T-5, respectively.

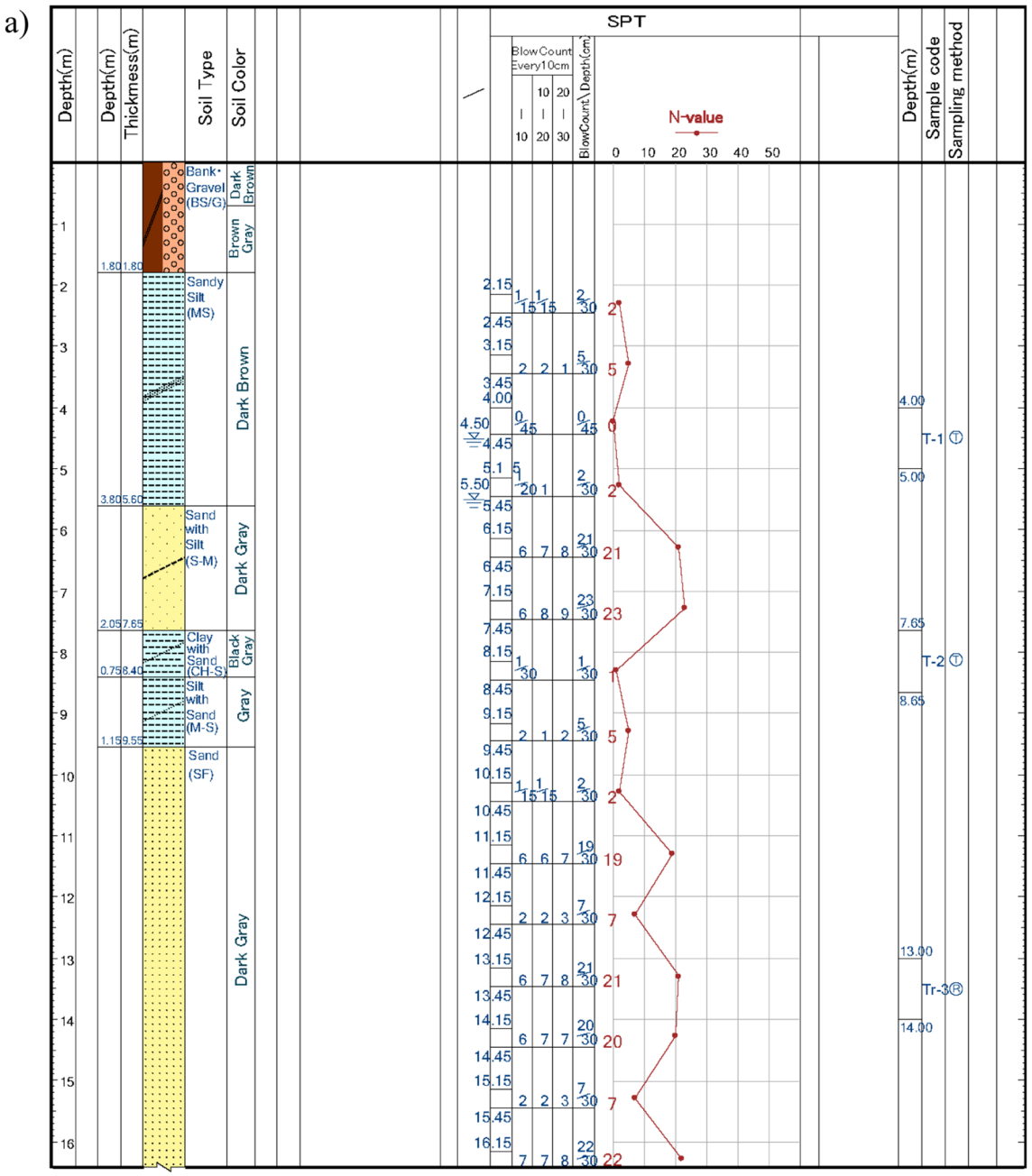

Fig. 3 Borehole log with N-values obtained from SPT. **a** Depth of 0 m to 16.3 m, **b** depth of 16 m to 39.44 m. The soil conditions shown in the far left of the figure are listed in Table 1. The upper 28 m is mostly sandy layers with N-values of about 20 or less, except between depths of 16 and 19 m where N-value becomes close to 30. The N-value becomes low again at about 22 m where there is a silt layer about 3 m thick. The sandy layer reappears down to 31 m where the gravel layer appears and the N-value reaches 50 at 33 m depth. The detailed depth locations of the samples T-1, T-2, Tr-3, Tr-4 and T-5 are shown on the far right of the figure and are presented in Table 3, Additional file 1: Tables S2 and S3. As for the sampling method, "T" stands for "thin-walled tube sampling" and "R" is for "rotary triple-tube sampling"

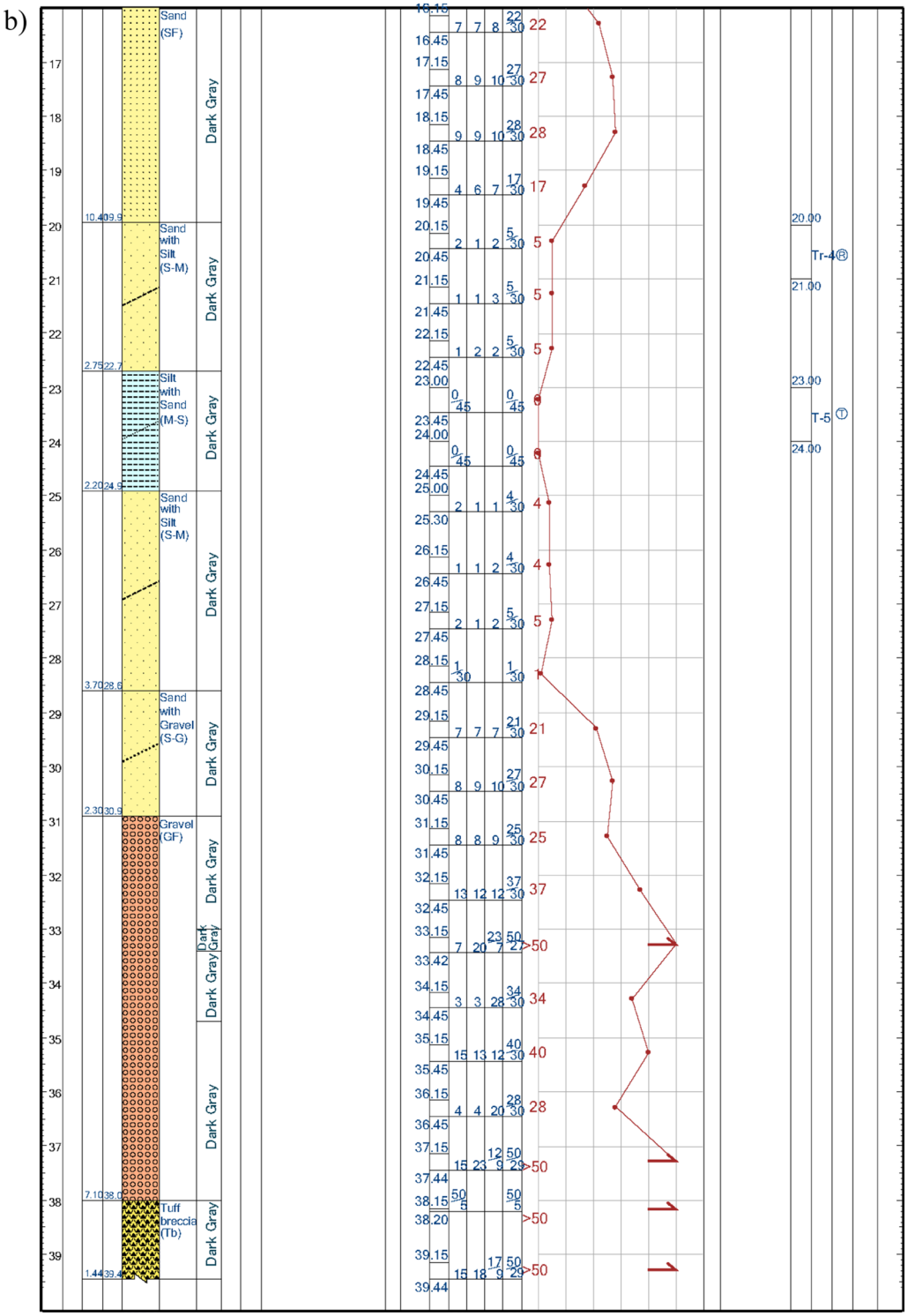

Fig. 3 continued

Data acquisition

Microtremor data

The microtremor measurements were performed for arrays of five different sizes (KUM-SS1, S, SM, M, LL). Each array consists of two equilateral triangles and seven sensors were used to observe microtremors simultaneously. The combination of the side lengths of the two triangles of each array are (1, 2), (10, 20), (39, 78), (122, 243),

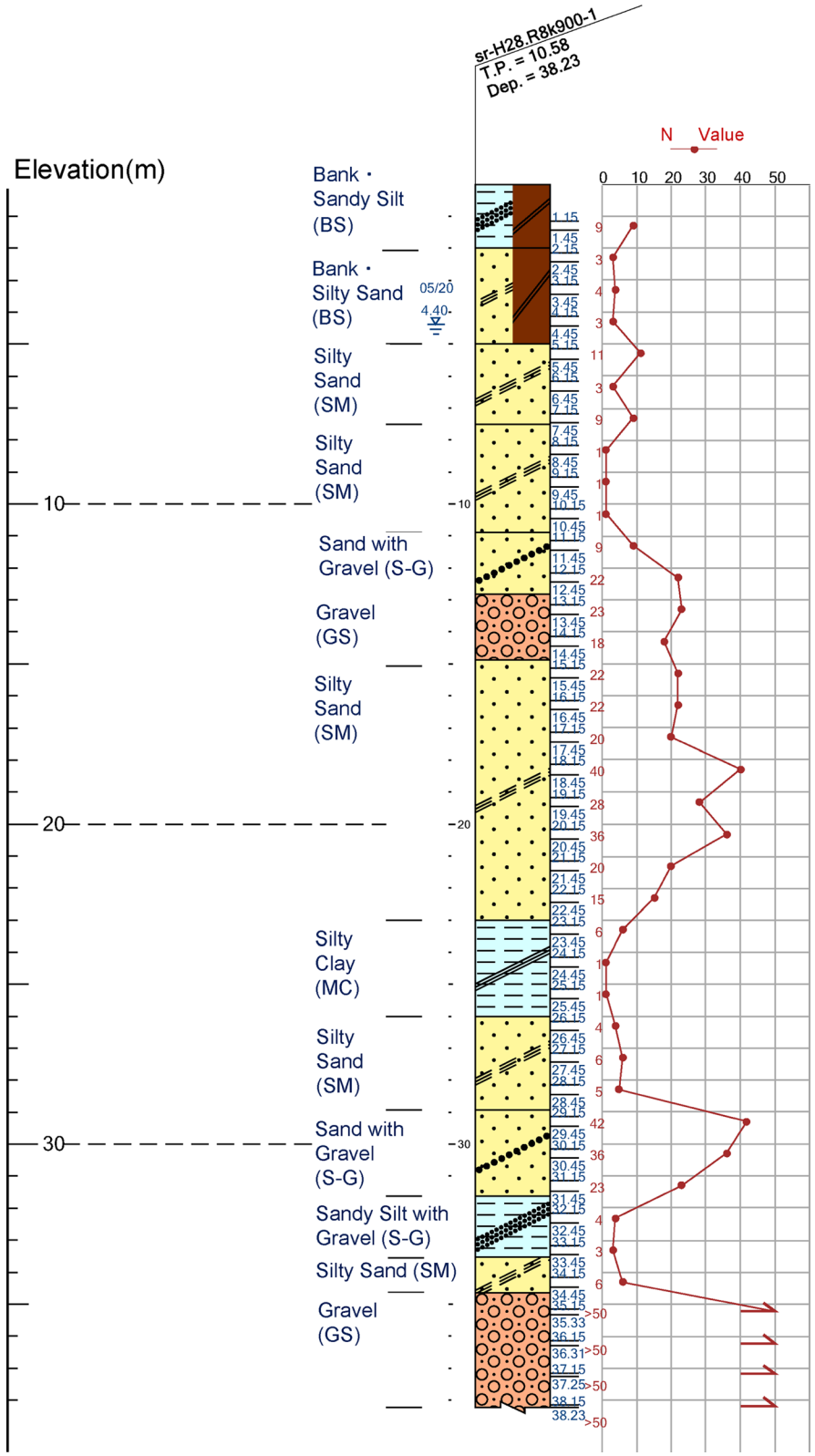

Fig. 4 Borehole log with N-values from SPT at a point south-east of KUMA, point "Shirakawa 2 No.1 (2) levee crown of right bank" made from information in Kuni-jiban (2022) (in the red circle of Fig. 2b)

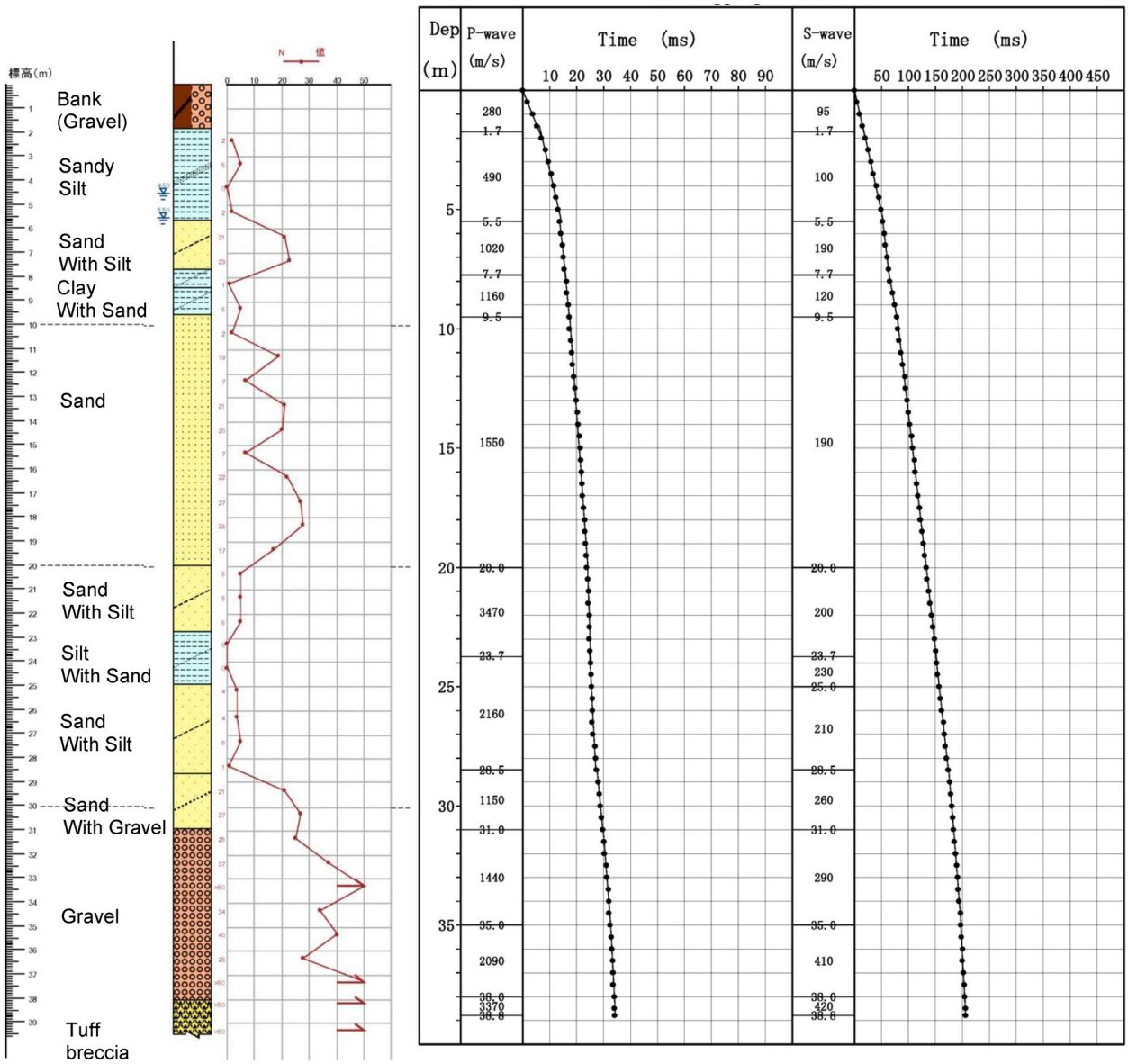

Fig. 5 PS logging results performed for every 0.5 m in depth, for the whole 39 m compared with layering obtained from the boring log in the left side of the figure. Data of P- and S- wave velocities are presented in Table 2

and (481, 962) in meters for arrays KUM-SS1, S, SM, M, and LL, respectively. The sensors used for the observation were SE-321 manufactured by Tokyo Sokushin, consisting of three components (UD, NS, and EW) with a natural period of 10 s and sensitivity of 5 V/(cm/s). The data logger used was an LS8800 manufactured by Hakusan Corporation. The sampling rate was 200 Hz with 24-bit accuracy. The dynamic range is 128 dB. Time correction was performed at every one hour during the measurements. The duration of the distributed data is 45 min for KUM-SS1 and 60 min for the other four arrays. The maps of the microtremor triangular arrays KUM-SS1&S, SM, M, and LL are shown in Additional file 1: Figure S5 and the locations of the triangular arrays KUM-SM, KUM-M and KUM-LL are shown in Additional file 1: Table S14.

Active source data for MASW

The active source measurement was conducted along a 36 m survey line approximately 30 m to 50 m west of KUMA, as shown in Fig. 8. Vertical geophones were distributed at 1.5 m intervals along the survey line (Fig. 8a). Data for 10 shots are collected for each shot-receiver

Table 1 Soil conditions of boring log, presented graphically in Fig. 3

Depth (m)	Thickness (m)	Soil type
1.80	1.80	Bank (gravel)
5.60	3.80	Sandy silt
7.65	2.05	Sand with silt
8.40	0.75	Clay with sand
9.55	1.15	Silt with sand
19.95	10.40	Sand
22.70	2.75	Sand with silt
24.90	2.20	Silt with sand
28.60	3.70	Sand with silt
30.90	2.30	Sand with gravel
38.00	7.10	Gravel
39.44	1.44	Tuff breccia

Table 2 Velocity profile obtained from P-S logging, presented graphically in Fig. 5

Depth (m)	Thickness (m)	P-wave velocity (m/s)	S-wave velocity (m/s)
1.7	1.7	280	95
5.5	3.8	490	100
7.7	2.2	1020	190
9.5	1.8	1160	120
20.0	10.5	1550	190
23.7	3.7	3470	200
25.0	1.3	2160	230
28.5	3.5	2160	210
31.0	2.5	1150	260
35.0	4.0	1440	290
38.0	3.0	2090	410
38.8	0.8	3370	420

gather. Shot points were located at either end of the survey line. A sledgehammer was used to create a vertical impact as an artificial source. Data were sampled at 1 kHz intervals. The north-east end of the survey line was approximately 10 m south-west of the borehole survey location as shown in Fig. 8b. The condition of the survey line is shown in Fig. 8c.

Earthquake ground motion data

Test site and reference site

The strong ground motions during the 2016 Kumamoto earthquake sequence, Japan, which occurred on April 14, 2016, at 21:26 JST (Japan Meteorological Agency (JMA) Magnitude (M_{JMA}) 6.5) and April 16, 2016, at 1:25 JST (M_{JMA} 7.3), and the weak ground motions during the aftershocks of these earthquakes were recorded at the Kumamoto test site without any publication. Also, the strong ground motions during the 2016 Kumamoto earthquake sequence and the weak ground motions during these aftershocks were recorded at the reference site (Tsuno et al. 2017). The test site KUMA, which was installed and maintained by JR Kyushu, is located on Quaternary layers in the northern part of the Kumamoto Plain, Japan. On the other hand, the reference site where the strong ground motion station (KU.KMP1) was installed and maintained by the Institute of Seismology and Volcanology, Faculty of Science, Kyushu University, is located on Mt. Kimbo, where tuff breccia is widely distributed (Hoshizumi et al. 2004). The locations of KUMA and KU.KMP1 are shown in Fig. 2 and Table 4.

Earthquake records

For the period of about two months after the 2016 Kumamoto earthquake sequence, earthquake records of two hundred earthquakes with M_{JMA} greater than 3 were observed including strong motions and week motions at KUMA. As the target earthquake in BP2, the largest aftershock of M_{JMA} 5.9 occurred on April 16, 2016, at 3:03 JST with Peak Ground Acceleration (PGA) of less than 50 cm/s^2 at KUMA was selected, and the target weak motion record (No.35 in Table 5) at KU.KMP1 was released. The velocities at KU.KMP1 for the largest aftershock of M_{JMA} 5.9 (the target earthquake) provided in BP2 are shown in Fig. 9a. As the target earthquakes in BP3, the foreshock of M_{JMA} 6.5 that occurred on April 14, 2016, at 21:26 JST and the mainshock of M_{JMA} 7.3 that occurred on April 16, 2016, at 1:25 JST were selected and the target strong motion records at KU.KMP1 were released. The velocities at KU.KMP1 for the foreshock of M_{JMA} 6.5 and the mainshock of M_{JMA} 7.3 (the target earthquakes) provided in BP3 are shown in Fig. 9b.

In addition, 12 weak motion records with epicenters widely distributed in the source fault planes of the foreshock and the mainshock of the 2016 Kumamoto earthquake sequence (Asano and Iwata 2016), were released for both KU.KMP1 and KUMA. The velocities at KU.KMP1 and accelerations at KUMA for the 12 aftershocks provided in BP2 are shown in Figs. 10 and 11, respectively. The PGA in the EW component during an earthquake of No.80 is only above 50 cm/s^2 with a sharp amplitude in the high frequency at the test site. The information and locations of the earthquakes provided in BP2 are shown in Table 5 and Fig. 2, respectively. The ground motions at KU.KMP1 were recorded by a velocity-meter and the ground motions at KUMA were recorded by an accelerometer, as shown in Table 4. The raw data (velocity at the reference site of KU.KMP1 and acceleration at the test site of KUMA), whose DC

Table 3 Specimen conditions and test results of the cyclic triaxial test to determine deformation properties of geomaterials

Sample no.	Depth	Consolidation pressure	Density of soil particles	Specimen status	Initial condition				Before consolidation		After consolidation		Test results			
					Wet density	Water content	Dry density	Void ratio	Dry density	void ratio	Dry density	Void ratio	E_0	ε_a	G_0	γ_r
	(m)	(kN/m^2)	(g/cm^3)		(g/cm^3)	(%)	(g/cm^3)		(g/cm^3)		(g/cm^3)		(MN/m^2)	(%)	(MN/m^2)	(%)
T-1	4.00 ~ 5.00	65	2.701	Bulk	1.367	125.9	0.605	3.464	0.608	3.442	0.638	3.236	31.7	1.01E-01	10.6	1.52E-01
T-2	7.65 ~ 8.65	90	2.479	Bulk	1.289	164.3	0.488	4.080	0.490	4.059	0.523	3.736	23.3	2.45E-01	7.8	3.67E-01
Tr-3	13.00 ~ 14.00	130	2.831	Frozen	1.912	25.9	1.519	0.864	1.536	0.843	1.558	0.817	170.7	4.48E-02	56.9	6.72E-02
Tr-4	20.00 ~ 21.00	200	2.782	Frozen	1.836	33.9	1.371	1.029	1.412	0.970	1.442	0.929	198.6	6.99E-02	66.2	1.05E-01
T-5	23.00 ~ 23.72	50	2.693	Bulk	1.501	86.3	0.806	2.341	0.807	2.337	0.850	2.168	94.7	1.34E-01	31.6	2.01E-01

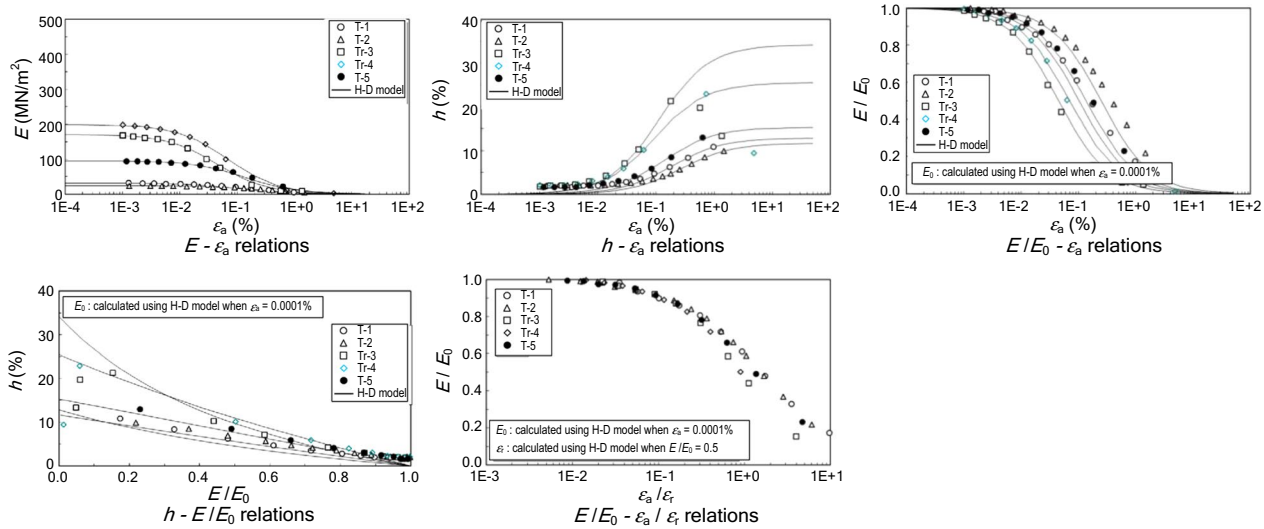

Fig. 6 Figures of Young's modulus—strain (E-ε_a) and hysteric damping—strain (h-ε_a) relationship of samples T-1 T-2, Tr-3, Tr-4 and T-5 obtained at the borehole site for laboratory tests shown. Data are presented in Additional file 1: Tables S4 to S8

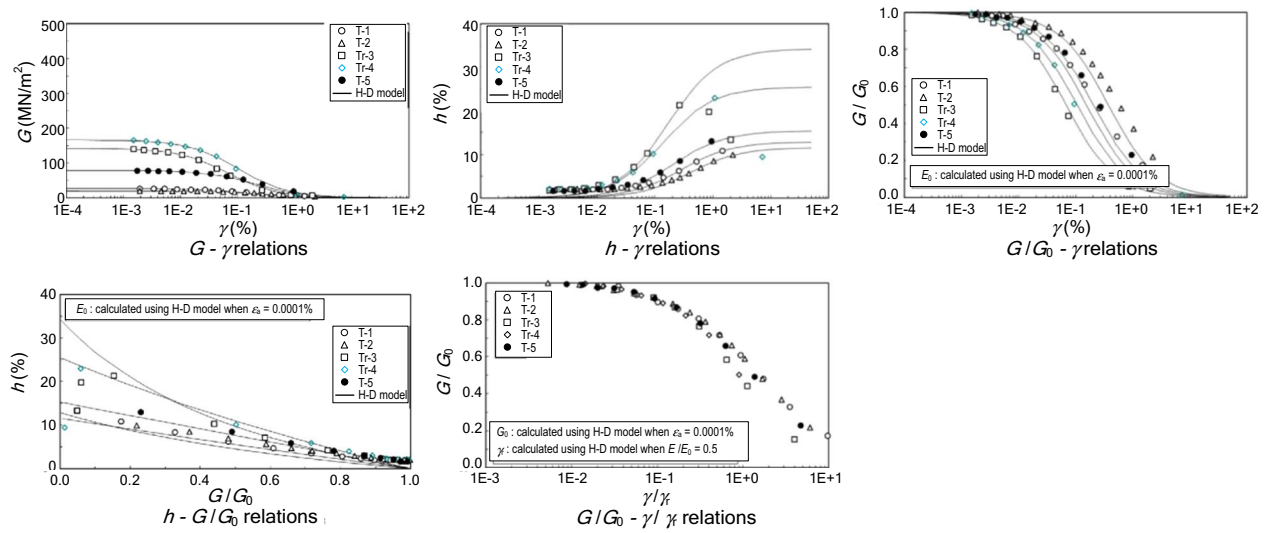

Fig. 7 Plots of shear modulus—shear strain (G-γ) and hysteric damping—shear strain (h-γ) relation of samples T-1 T-2, Tr-3, Tr-4 and T-5 obtained at the borehole site for laboratory tests. Data are presented in Additional file 1: Tables S9 to S13

components were extracted by using the average over the whole duration of each recording were offered, without any other corrections.

Additional information

The results of in situ measurements and laboratory tests, the preferred 1-D velocity model by the ESG6 local organizing committee were provided, as follows in (1) and (2). The information on the Japan Integrated Velocity Structure Model (JIVSM) and the geological map around KUMA released by the National Institute of Advanced Industrial Science and Technology (AIST), were provided, as shown in (3) and (4):

(1) The results of in situ measurements and laboratory tests were reported as in the "Site information" section.
(2) The preferred velocity model was constructed by the ESG local organizing committee as in the "Preferred velocity model" section.
(3) JIVSM was constructed by Koketsu et al. (2009, 2012), and descriptions in English were distributed.

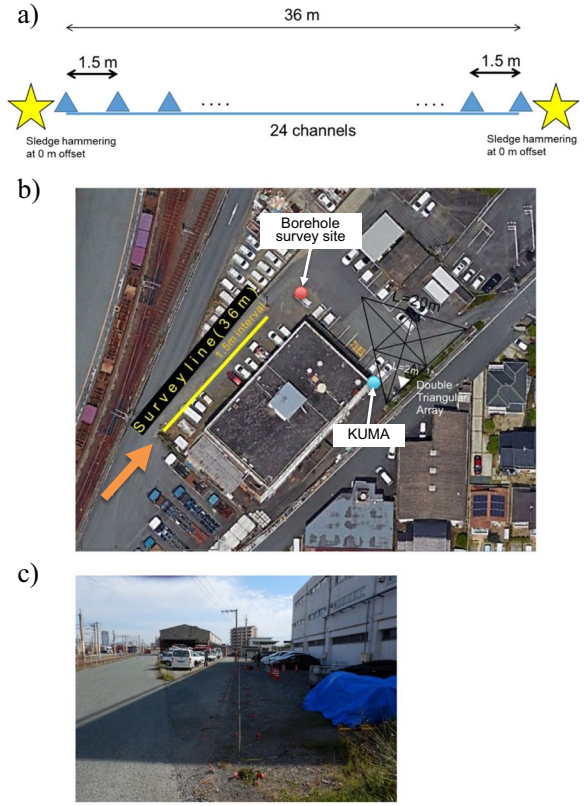

Fig. 8 **a** Active source measurement configuration. The star indicates the shot point and triangles indicate the location of the geophones. **b** Location of the survey line (yellow line) of the active source measurement along with the borehole site (red circle) and KUMA site (blue circle), plotted on Google Map, **c** photo taken from the south side of the survey line indicated by an orange arrow in **b**

(4) The Seamless Digital Geological Map of Japan (1:200,000) by AIST was introduced as the reference geological map.

Preferred velocity model

Construction of a 1-D profile

A preferred velocity model constructed at KUMA using available subsurface velocity data to provide to BP2 and BP3 participants for the use in the blind prediction tests after the BP1 results were submitted. The preferred velocity model is a 1-D profile of velocities of P- and S-waves, densities for the shallow and deep sedimentary layers over the basement with an S-wave velocity greater than 3 km/s.

The shallow part of the preferred velocity model was derived from the result of the P-S logging at the strong motion site. The top 10 layers above the engineering bedrock with S-wave velocity greater than 400 m/s in the logging profile are also included in the preferred velocity model. The same physical parameters as in the logging were used for the 10 layers, including their thicknesses.

The deep part of the preferred velocity model was based on the structural data available in the previous surveys. Figure 12a shows three 1-D S-wave profiles obtained from the existing 3-D velocity models around the KUMA station. JIVSM is a 3-D velocity model constructed by compiling geological and geophysical data with earthquake records of moderate events (Koketsu et al. 2012). This model has a top layer with an S-wave velocity of 350 m/s. The Japan Seismic Hazard Information Station (J-SHIS, Ver 2) also provides a 3-D velocity model for most of Japan (NIED 2018). The 1-D velocity model of J-SHIS has an upper layer with an S-wave velocity of 650 m/s. The depth to the basement with an S-wave velocity of about 3 km/s in the J-SHIS model is deeper than that of JIVSM. Most of the S-wave velocities of the sediments in the J-SHIS model are also higher than those in JIVSM. These two models were constructed to simulate long-period ground motions on a regional scale. However, Senna et al (2018) conducted microtremor surveys in Kumamoto Plain and Mt. Aso to construct a 3-D velocity model. A 1-D profile obtained at KUMA from the 3-D model by Senna et al. (2018) is shown in Fig. 12a. This model includes shallow and deep portions of sedimentary layers with S-wave velocities ranging from 170 to 3200 m/s. The S-wave distribution of the deep part of this model is similar to that of JIVSM.

The performance of the three models was examined by comparison with Rayleigh wave phase velocities derived from measurements at the KUMA station. The array

Table 4 Information of strong ground motion stations at the test site of KUMA and the reference site of KU.KMP1

Station code	Longitude	Latitude	Height (m)	Geological condition	Seismometer
KUMA	130.6879	32.7756	10.0	Quaternary layer	Accelerometer (STR-361, Takamisawa Cybernetics Co., Ltd.)
KU.KMP1	130.6227	32.8198	175.0	Andesite	Velocity-meter (VSE-11F/12F, Tokyo Sokushin Co., Ltd.)

Table 5 Information by JMA and F-net on earthquakes provided in the blind predictions (BP2 and BP3) shown by circles and a star in Fig. 2a

No.	JMA										F-net							
	Y	M	D	H	M	S	Latitude	Longitude	Depth (km)	M	Latitude	Longitude	Depth (km)	Strike (°)	Dip (°)	rake (°)	M_0 (Nm)	M_w
4	2016	4	16	1	5	42.48	32.71633	130.80483	15.46	3.3	No information							
35	2016	4	16	3	3	10.78	32.96383	131.08683	6.89	5.9	32.9638	131.0868	5	209; 116	60; 85	− 174; − 30	1.92E + 17	5.5
43	2016	4	16	4	5	49.2	32.79733	130.81317	12.29	4.0	No information							
64	2016	4	16	7	23	54.32	32.78667	130.77383	11.93	4.8	32.7867	130.7738	5	92; 248	29; 63	− 69; − 101	8.86E + 15	4.6
80	2016	4	16	11	2	51.71	32.75833	130.77817	14.57	4.4	32.7583	130.7782	11	199; 34	41; 50	− 102; − 80	3.72E + 15	4.3
104	2016	4	17	0	14	51.69	32.96167	131.07917	8.92	4.8	32.9617	131.0792	8	241; 140	54; 75	− 161; − 38	1.18E + 16	4.7
109	2016	4	17	4	46	49.09	32.68717	130.77617	10.32	4.5	32.6872	130.7762	5	276; 181	60; 82	10; 150	4.52E + 15	4.4
121	2016	4	17	19	23	41.22	32.6775	130.72067	10.58	4.4	32.6775	130.7207	8	302; 80	39; 59	− 55; − 115	4.88E + 15	4.4
127	2016	4	18	8	35	43.02	32.8695	130.87333	10.2	4.2	32.8695	130.8733	8	318; 98	36; 61	− 56; − 112	2.41E + 15	4.2
161	2016	4	21	21	52	3.39	32.78533	130.83183	10.98	4.0	32.7853	130.8318	8	358; 262	65; 78	− 167; − 26	7.14E + 14	3.9
205	2016	5	5	10	31	30.47	33.0003	131.13417	11.16	4.6	33.0003	131.1342	8	208; 116	71; 84	− 174; − 19	8.44E + 15	4.6
206	2016	5	5	10	40	12.83	32.99283	131.12217	10.81	4.9	32.9928	131.1222	8	320; 228	79; 84	6; 169	1.52E + 16	4.8
227	2016	5	19	2	37	44.28	32.83133	130.81417	16.43	3.9	No information							

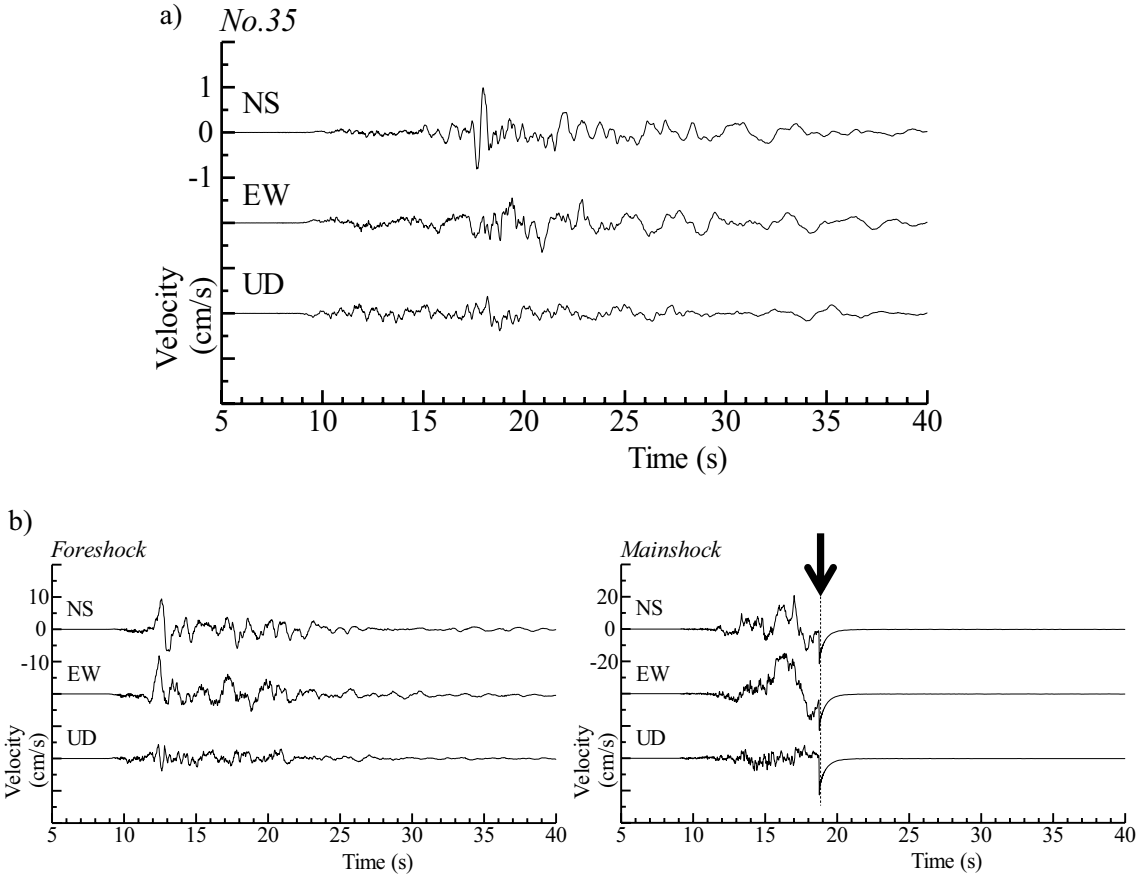

Fig. 9 **a** Velocity waveforms at KU.KMP1 for the largest aftershock of M_{JMA} 5.9 (the target earthquake) provided in BP2. In the figure, waveforms start on April 16, 2016, at 3:03:10 JST. **b** Velocity waveforms at KU.KMP1 for the foreshock of M_{JMA} 6.5 and the mainshock of M_{JMA} 7.3 (the target earthquakes) provided in BP3. In the figure of the foreshock, waveforms start on April 14, 2016, at 21:26:30 JST. In the figure of the mainshock, waveforms start on April 16, 2016, at 1:25:00 JST. At the time of the arrow, the power was shutdown at KU.KMP1 and no data were recorded after this time

records of vertical microtremors used in BP1 were used to obtain the Rayleigh wave phase velocity over a wide frequency range. The phase velocity was submitted to the blind test by some of the authors before the preferred velocity model was determined. The theoretical phase velocities of the fundamental Rayleigh waves in the three models are shown in Fig. 12b together with the observed ones. The models of JIVSM and Senna et al. (2018) show a high similarity with the observed phase velocity. In particular, the theoretical phase velocity for the model of Senna et al. (2018) agrees with the observation in a wide frequency range. Since the velocity model of Senna et al. (2018) was mainly built with Rayleigh wave phase velocity data from microtremor surveys in the area around the KUMA station, this high agreement of the phase velocities is quite understandable. Therefore, the 1-D velocity model of Senna et al. (2018) was used for the deep part of the preferred velocity model.

The layers below the layers with having an S-wave velocity of 400 m/s in the 1-D velocity model by Senna et al. (2018) are included at the bottom of the above shallow part for the preferred velocity model of shallow and deep sedimentary layers at KUMA station. The constructed preferred profile is shown in Fig. 12c and tabulated in Table 6.

Validation of the 1-D profile

We have validated the constructed preferred velocity model by comparing it to the earthquake records provided in the second and third steps of the blind test. 10 weak motion records at the target and rock sites in the blind test were used in the validation. We calculated ratios of S-wave spectra from the records at KUMA to half of those at the rock site KU.KMP1 as an assumed incident wave to account for the free surface condition at KU.KMP1. The averaged ratios were compared with theoretical amplification factors of the vertical 1-D

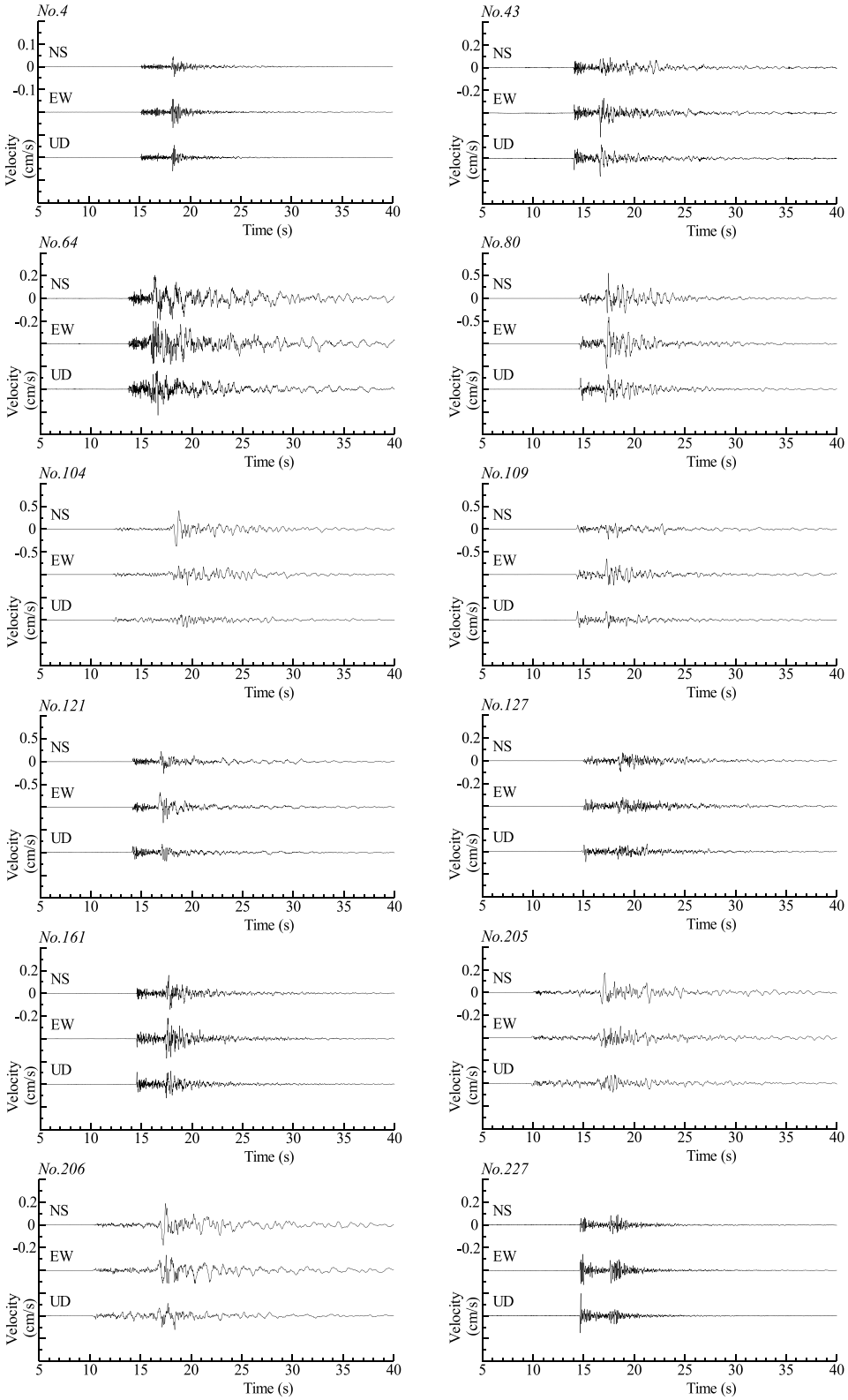

Fig. 10 Velocity waveforms at KU.KMP1 for the aftershocks provided in the blind predictions (BP2 and BP3)

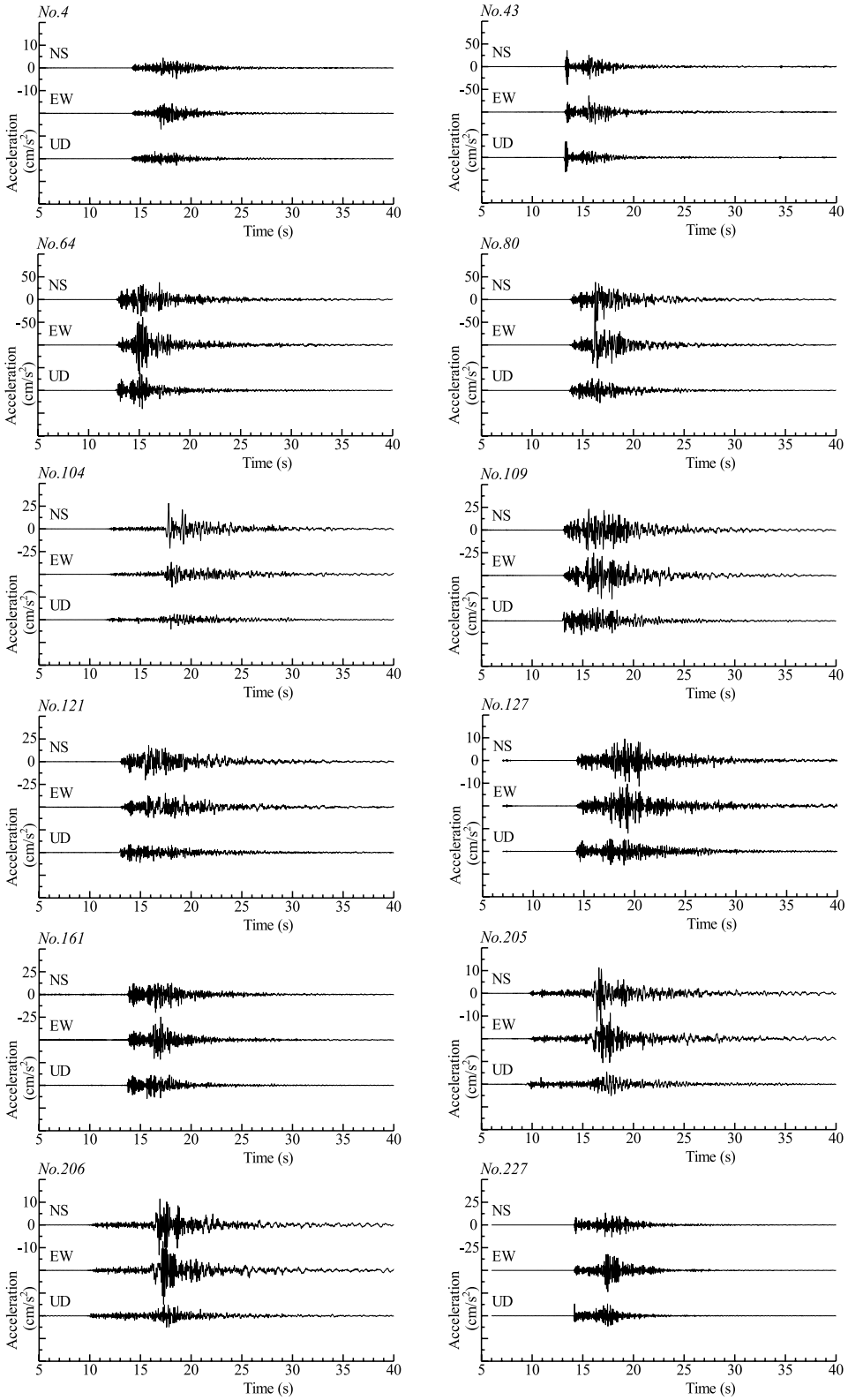

Fig. 11 Acceleration waveforms at KUMA for the aftershocks provided in the blind predictions (BP2 and BP3)

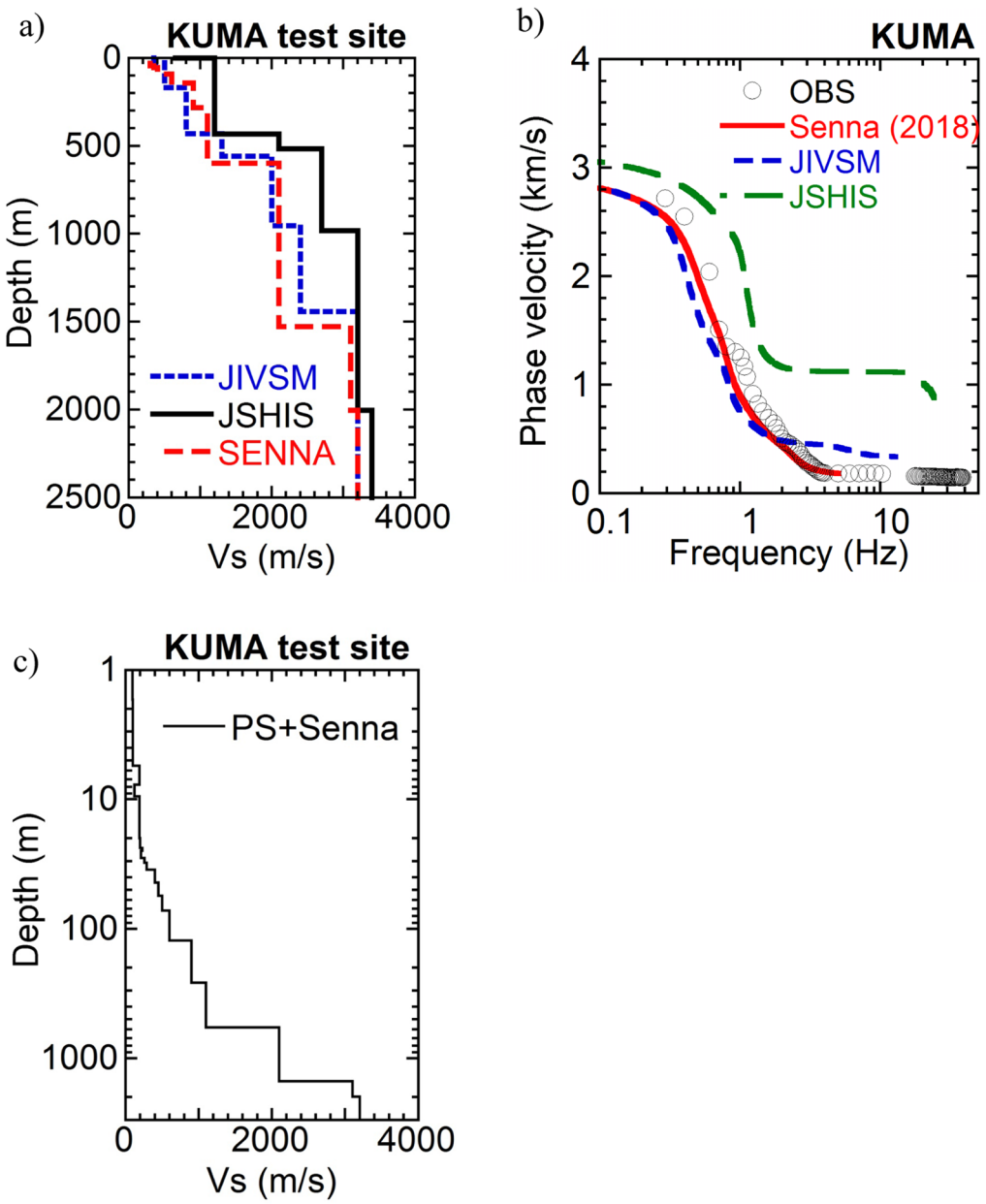

Fig. 12 **a** S-wave velocity profiles at KUMA in existing 3-D models of deep sedimentary layers. Black, blue and red lines indicate 1D S-wave velocity distributions extracted from J-SHIS (NIED, 2019), Koketsu et al. (2009) and Senna et al. (2018). **b** Comparison of observed Rayleigh-wave phase velocities (circles) and theoretical ones for S-wave models (lines) in a). Green, blue and red lines indicate 1D S-wave velocity distributions extracted from J-SHIS (NIED, 2019), Koketsu et al. (2009) and Senna et al. (2018). **c** 1-D S-wave velocity profile of shallow and deep sedimentary layers at KUMA as the "preferred velocity model" in the blind test in ESG6. The shallow part of the profile was constructed from results of S-wave velocity at borehole, while the deep part was imported from Senna et al. (2018)

S-wave in the preferred velocity model. Q-value of each layer was assumed to be equal to one-tenth of the S-wave velocity in m/s according to previous studies (e.g., Olsen et al 2003; Zhu et al. 2022). Figure 13 shows the observed spectral ratios with the calculated amplification for the preferred velocity model. Since the measured S-wave distribution at the rock site is not known, three amplification factors were calculated for the layers above the layers with S-wave velocities of 3200, 2100, 1100 m/s for comparison. The observed ratio is very similar to the amplification factor for the layers above the layer with an S-wave velocity of 1100 m/s in the 0.5 to 10 Hz frequency range,

Table 6 Velocity profile of the constructed "preferred velocity model", presented graphically in Fig. 12c

Layer no.	Vp (m/s)	Vs (m/s)	Density (g/cm^3)	Thickness (m)
1	280	95	1.50	1.70
2	490	100	1.50	3.80
3	1020	190	1.60	2.20
4	1160	120	1.50	1.80
5	1550	190	1.60	10.50
6	3470	200	1.70	3.70
7	2160	230	1.70	1.30
8	2160	210	1.70	3.50
9	1150	260	1.70	2.50
10	1440	290	1.70	4.00
11	1600	400	1.85	8.96
12	1600	450	1.85	11.84
13	1700	500	1.90	16.56
14	2100	600	1.90	51.07
15	2400	900	2.05	138.67
16	2600	1100	2.15	317.82
17	4000	2100	2.40	929.16
18	5500	3100	2.60	475.57
19	5500	3200	2.65	–

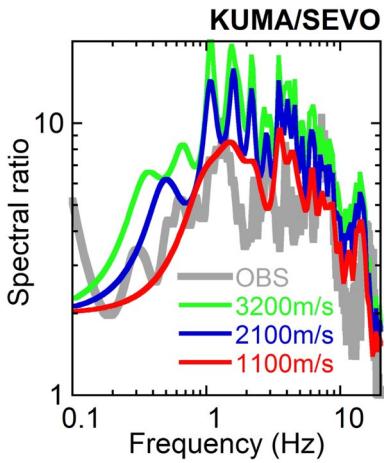

Fig. 13 Observed spectral ratios between KUMA and KU.KMP1 (gray line) compared with calculated amplification from layers of Vs = 1100 m/s, Vs = 2100 m/s and Vs = 3200 m/s in red, blue and green lines, respectively, to the surface of the preferred velocity model

providing sufficient validation of the preferred velocity model for the use in the ground motion simulations. The other amplification factors are larger than the observed ratio throughout the entire frequency range. This indicates that the subsurface structure at the rock site may contain the layer with an S-wave velocity of 1100 m/s, and the effects of layers deeper than this layer are common between KU.KMP1 and KUMA. Actual velocity data at KU.KMP1 are required for a quantitative interpretation of the observed spectral ratio.

Conclusions

A brief introduction of the history of 35 years of JWG-ESG and the history of five ESG symposia that were held in Odawara, Yokohama, Grenoble, Santa Barbara and Taipei, that since 1992 and the blind predictions and simultaneous simulations conducted for these symposia were summarized. The outline of ESG6 and the blind prediction exercise for ESG6 were introduced.

The location of the target test site for the BP of ESG6, KUMA is a strong motion observation site located in Kumamoto City, Kumamoto, Japan, in the northern part of the Kumamoto Plain. The characteristics of the strong ground motion during the 2016 Kumamoto earthquake near JR Kumamoto Station, which is about 1 km north of KUMA, has been studied, but the ground motion records at the target test site was undisclosed until ESG6. Preliminary microtremor observations were made at KUMA and found that there is no strong lateral heterogeneity in and around the site. There is a nearby rock site KU.KMP1, operated by Kyushu University about 10 km north-west of KUMA, and its ground motion records were provided to the participants to be used as a reference.

In order to investigate the subsurface structure of the target site of the blind prediction exercise, a thorough investigation including several types of surveys was conducted in and around the target site.

The information on the microtremor observations and active source measurements that were conducted near the target test site KUMA to collect data for the BPs was described in detail. The data obtained from these observations and additional information distributed to the BP1 participants were explained. The microtremor observation was performed for longer duration compared to the duration often performed for practice. Also, the observations for large radius arrays were conducted overnight. These measures made the data more stable and reliable, leading to stable results in BP1.

On the other hand, information about the ground motion data collected at KUMA and KU.KMP1 and information about the related seismic sources were compiled from existing literature and presented to the participants of BP2 and BP3.

In addition, the results of the borehole survey conducted at a site near KUMA to obtain information to verify the results submitted by the participants of the BP of ESG6 were presented. This includes information such as the results of the in situ measurements including P-S logging and laboratory tests of the five samples

collected at the borehole survey site. P-S logging was done for every 0.5 m, which is more detailed compared to the P-S logging done for practice, which is done for every 1 m or more. This allowed a detailed comparison with the phase velocity and velocity structure estimated by the BP participants.

Finally, the approach and procedure for constructing the "preferred velocity model" provided to the participants was explained in detail. We constructed a velocity profile of the shallow and deep sedimentary layers from a combination of the geophysical and geotechnical data at the site, and validated it by comparing the characteristics of the ground motion data from the moderate event. The amplification factor calculated from the "preferred velocity model" showed that the amplification factor from the Vs = 1100 m/s layer was consistent with the observed amplification factor. This "preferred velocity model" was provided as a standard model to the participants of the second and third steps of the blind prediction test to predict the earthquake ground motions of a moderate event and the mainshock of the 2016 Kumamoto earthquake.

Abbreviations

AIST	National Institute of Advanced Industrial Science and Technology
BP	Blind prediction exercise
BP1	Step 1 of BP
BP2	Step 2 of BP
BP3	Step 3 of BP
CDMG	California Division of Mines and Geology
DPRI	Disaster Prevention Research Institute, Kyoto University
ERI	Earthquake Research Institute, University of Tokyo
ESG	Effect of Surface Geology on Seismic Motion
ESG1 to ESG6	The First to Sixth IASPEI/IAEE International Symposium on ESG
IAEE	International Association of Earthquake Engineering
IASPEI	International Association of Seismology and Physics of the Earth's Interior
JAEE	Japan Association for Earthquake Engineering
JIVSM	Japan Integrated Velocity Structure Model
JR	Japan Railway
J-SHIS	Japan Seismic Hazard Information Station
JWG-ESG IASPEI/IAEE	Joint Working Group on Effects of Surface Geology on Seismic Motion
MASW	Multi-channel Analysis of Surface Waves
NIED	National Research Institute for Earth Science and Disaster Resilience
PGA	Peak ground acceleration

Supplementary Information

The online version contains supplementary material available at https://doi.org/10.1186/s40623-024-01958-0.

Additional file 1: Table S1. Standards of laboratory tests. **Table S2.** Summary of results of laboratory tests. **Table S3.** Particle size distribution of soils for each sample. **Table S4.** *E*-ε_a, *h*-ε_a relation of sample T-1, presented graphically in Figure 6. **Table S5.** *E*-ε_a, *h*-ε_a relation of sample T-2, presented graphically in Figure 6. **Table S6.** *E*-ε_a, *h*-ε_a relation of sample Tr-3, presented graphically in Fig. 6. **Table S7.** *E*-ε_a, *h*-ε_a relation of sample Tr-4, presented graphically in Fig. 6. **Table S8.** *E*-ε_a, *h*-ε_a relation of sample T-5, presented graphically in Fig. 6. **Table S9.** *G*-γ, *h*-γ relation of sample T-1, presented graphically in Fig. 7. **Table S10.** *G*-γ, *h*-γ relation of sample T-2, presented graphically in Fig. 7. **Table S11.** *G*-γ, *h*-γ relation of sample Tr-3, presented graphically in Fig. 7. **Table S12.** *G*-γ, *h*-γ relation of sample Tr-4, presented graphically in Fig. 7. **Table S13.** *G*-γ, *h*-γ relation of sample T-5, presented graphically in Fig. 7. **Table S14.** Location of microtremor triangular arrays of KUM-SM, KUM-M and KUM-LL, shown in Figure S5. **Figure S1.** The conditions of the strong motion observation sites a) KUMA and b) KU.KMP1. **Figure S2.** The accelerometer that recorded the ground motion at KUMA. a) Location of the observation case, b) Inside the observation case. **Figure S3.** P-wave waveform of the PS logging. **Figure S4.** S-wave waveform of the PS logging. **Figure S5.** Maps of microtremor triangular arrays of a) KUMA-SS1 (1, 2) and KUMA-S (10, 20), b) KUMA-SM (39, 78), c) KUMA-M (122, 243), and d) KUMA-LL (481, 962). The numbers in the parentheses are side lengths of the two triangles in the array in meters. a) plotted on Google Map and b) to d) plotted on Google Earth.

Acknowledgements

The concept building of BPs for ESG6 and the preparation and management of the BPs were conducted by the working groups (WGs) for modelling the preferred velocity model (WG-PM) and for analysis and selection of ground motion data (WG-GM), of the ESG6 local organizing committee. The borehole survey, microtremor observations and active source measurements were conducted on the premises of an affiliate of JR Kyushu. These surveys could not have been possible without the cooperation of JR Kyushu and its affiliate. The borehole survey and laboratory tests were conducted by OYO Corporation. The microtremor data were collected with the cooperation of Dr. Takeshi Sugiyama and Dr. Masayuki Yoshimi of AIST. The digital data of the velocity model of Senna et al. (2018) were provided by Dr. Shigeki Senna of NIED. The digital data of JIVSM and its English explanation were provided by Prof. Kazuki Koketsu of Keio University and Prof. Hiroe Miyake of ERI. Ground motion data observed at KU.KMP1 were provided by Kyushu University. Ground motion data observed at KUMA were provided by JR Kyushu. The authors would like to express their special appreciation to these collaborators who provided the digital data. The authors also thank all members of the ESG6 local organizing committee and the members of the research committee on strong motion evaluation of JAEE for their support and cooperation in conducting the surveys. The members of the WG-PM were Prof. Hiroaki Yamanaka, Dr. Shigeki Senna, Dr. Takumi Hayashida of Building Research Institute, Dr. Shusuke Oji of Chuo Kaihatsu Corporation and Dr. Yoshiaki Inagaki of OYO Corporation. The members of WG-GM- were Prof. Hiroshi Kawase, Dr. Seiji Tsuno, Dr. Takashi Hayakawa of Shimizu Corporation, Dr. Kazuhiro Kaneda of Chiba Institute of Technology, Dr. Tomonori Ikeura of Kajima Corporation, Prof. Tomotaka Iwata of Kyoto University and Dr. Shinako Noguchi of Association for the Development of Earthquake Prediction.

Author contributions

The structure of the manuscript was decided by SM, YH, ST and KC. Each author took part in organizing the content of the manuscript. SM edited sections "Introduction", "Blind Prediction exercise" and "Site information" with the help of YH, ST, KC, HS, HK and TM. SM and HS complied the information about the borehole survey. KC compiled the information about BP1. ST compiled the information about BP2&3. YH compiled the information about the "Preferred Velocity Model". SM drafted the original manuscript. All authors reviewed the manuscript draft and revised it critically. All authors approved the final version of the manuscript to be published.

Funding

The survey was funded by the Core-to-Core Collaborative Research between Earthquake Research Institute, The University of Tokyo and Disaster Prevention Research Institute, Kyoto University for FY2019, FY2020, FY2021 and FY2022.

Availability of data and materials

We provide digital data of microtremors and weak and strong ground motions released in these blind predictions on the website of JAEE, which was the main sponsor of ESG6. The location of the website is "https://www.jaee.gr.jp/en/2023/10/25/1741/". The datasets generated and/or analyzed in the current

study are not publicly available, but are available from the corresponding author upon reasonable request.

Declarations

Ethics approval and consent to participate
Not applicable.

Consent for publication
Not applicable.

Competing interests
Not applicable.

Author details
[1]Disaster Prevention Research Institute, Kyoto University, Gokasho, Uji, Kyoto 611-0011, Japan. [2]Tokyo Institute of Technology, 4259 Nagatsuta, Midori-ku, Yokohama, Kanagawa 227-8503, Japan. [3]Railway Technical Research Institute, 2-8-38 Hikari-cho, Kokubunji-shi, Tokyo 185-5840, Japan. [4]Kagawa University, 2217-20 Hayashi-cho, Takamatsu, Kagawa 761-0396, Japan. [5]OYO Corporation, Ginza Yamato 3 Building 4th Floor, 1-10-2 Sakuragi-cho, Omiya-ku, Saitama-shi, Saitama 330-0854, Japan. [6]Kyushu University, 2-5643-29 Shin'yama, Shimabara, Nagasaki 855-0843, Japan.

Received: 29 September 2022 Accepted: 5 January 2024
Published online: 15 March 2024

References

Asano K, Iwata T (2016) Source rupture processes of the foreshock and mainshock in the 2016 Kumamoto earthquake sequence estimated from the kinematic waveform inversion of strong motion data. Earth, Planets and Space 68:147. https://doi.org/10.1186/s40623-016-0519-9

California Division of Mines and Geology (CDMG) (1988) Proc. IASPEI/IAEE JWG ESG Workshop, XIX Assembly IUGG (1987), Tech. Rep. 88–1

Chaljub, E., C. Cornou, and P.-Y. Bard (2009). Numerical benchmark of 3D ground motion simulation in the valley of Grenoble, French Alps, in ESG 2006, Third Intl. Symposium on the Effects of Surface Geology on Seismic Motion, P.-Y. Bard, E. Chaljub, C. Cornou, F. Cotton, and P. Guéguen (Editors), LCPC Editions, ISSN 1628–4704, Vol.2: 1365–1375

Chimoto K, Tsuno S, Yamanaka H, Matsushima S, Kawase H, Takai N, Kanno T, Sato H, Shigefuji M, Korenaga M, Yamada N, Miyake H, Koketsu K, Asano K, Iwata T (2020) Ground motion observation and ground investigation at ESG6 blind prediction site. DPRI Annual Meeting 2020:P10

Chimoto K, Yamanaka H, Tsuno S, Matsushima S (2023) Predicted results of the velocity structure at the target site of the blind prediction exercise from microtremors and surface wave method as Step-1, -Report of the experiments for the 6th international symposium on effects of surface geology on seismic motion. Earth Planets Space 75:79. https://doi.org/10.1186/s40623-023-01842-3

Cornou C, Ohrnberger M, Boore D, Kudo K, Bard P-Y (2009) Derivation of structural models from ambient vibration array recordings: results from an international blind test. ESG2006, Third Intl. Symposium on the Effects of Surface Geology on Seismic Motion, P.-Y. Bard, E. Chaljub, C. Cornou, F. Cotton, and P. Guéguen (Editors), LCPC Editions, ISSN 1628–4704, Vol.2: 1127–1219

Hoshizumi H, Ozaki M, Miyazaki K, Matsuura H, Toshimitsu S, Uto K, Uchiumi S, Komazawa M, Hiroshima T, Sudo S (2004) Geological map of Japan 1:200,000, Kumamoto. Geological Survey of Japan, AIST

Iwata T, Sekiguchi H, Irikura K, Kawase H, Matsushima S (1999) Strong motion data and geological structures distributed for simultaneous simulation for Kobe. In: Irikura K et al. (eds) Proceedings of 2nd IASPEI/IAEE International Symposium, The Effect of Surface Geology on Seismic Motion, Balkema, Rotterdam, 3:1295–1310

JWG-ESG (1992) Proceedings of the Intern. Symp. on the ESG, Vol. I, II, III, Odawara Japan, March 25–27

Kawase H, Iwata T (1999) A report on submitted results of the simultaneous simulation for Kobe, In: Irikura K et al (eds) Proceedings of 2nd IASPEI/IAEE International Symposium, The Effect of Surface Geology on Seismic Motion, vol 3. Balkema, Rotterdam, pp 1311–1337

Koketsu K, Miyake H, Afnimar TY (2009) A proposal for a standard procedure of modeling 3-D velocity structures and its application to the Tokyo metropolitan area. Japan, Tectonophysics 472:290–300. https://doi.org/10.1016/j.tecto.2008.05.037

Koketsu K, Miyake H, Suzuki H (2012) Japan Integrated Velocity Structure Model Version 1, Proceedings of the 15th World Conference on Earthquake Engineering, Lisbon, Portugal, Oct. 12–17, Paper No. 1773

Kudo K, Sawada Y, (1992) Blind prediction experiments at Ashigara Valley, Japan. In: Proceedings of 10th World Conference on Earthquake Engineering, Balkema, Rotterdam, ISBN 90 5410 060 5, 6967–6971, Madrid, Spain

Kudo K (1992) Earthquake motions: Given and blinded data. In: Proceedings of 1st IASPEI/IAEE International Symposium on the Effects of Surface Geology on Seismic Motion vol 2. Odawara, Assoc Earthq Disaster Prevention, Japan, pp 53–60

Kudo K (2021) Background and additional notes on the establishment of JWG-ESG, Bulletin of JAEE No.43

Kuni-jiban (2022) Web search system for National land subsoil information, https://www.kunijiban.pwri.go.jp. Accessed 23 Sep 2022

Midorikawa S (1992) A statistical analysis of submitted predictions for the Ashigara Valley blind prediction test. In: Proceedings of 1st IASPEI/IAEE International Symposium on the Effects of Surface Geology on Seismic Motion, vol 2. Odawara, Assoc Earthq Disaster Prevention, Japan, pp 65–77

National Research Institute for Earth Science and Disaster Resilience (NIED) (2019) Japan Seismic Hazard Information System (J-SHIS) Velocity Profile Version 2, http://www.j-shis.bosai.go.jp/map/?lang=en. Accessed 1 Jul 2019

Olsen K, Day S, Bradley C (2003) Estimation of Q for Long-Period (>2 sec) Waves in the Los Angeles Basin. Bull Seismol Soc Am 93(2):627–638. https://doi.org/10.1785/0120020135

Senna S, Wakai A, Suzuki H, Yatagai A, Matsuyama H, Fujiwara H (2018) Modeling of the Subsurface Structure from the Seismic Bedrock to the Ground Surface for a Broadband Strong Motion Evaluation in Kumamoto Plain, Journal of Disaster Research 13:5 Special Issue on NIED Frontier Research on Science and Technology for Disaster Risk Reduction and Resilience 2018. https://doi.org/10.20965/jdr.2018.p0917

The Japanese Geotechnical Society (2015) Japanese geotechnical society standards laboratory testing standards of geomaterials (Vol.1).

The Japanese Geotechnical Society (2017) Japanese geotechnical society standards laboratory testing standards of geomaterials (Vol.2).

Tsuno S, Korenaga M, Okamoto K, Yamanaka H, Chimoto K, Matsushima T (2017) Local site effects in Kumamoto city revealed by the 2016 Kumamoto earthquake. Earth Planets Space 69:37. https://doi.org/10.1186/s40623-017-0622-6

Tsuno S, Nagashima F, Kawase H, Yamanaka H, Matsushima S (2023) Predicted results of the weak and strong ground motions at the target site of the blind prediction exercise as step-2 and -3, -report of the experiments for the 6th international symposium on effects of surface geology on seismic motion. Earth Planets Space 75:130. https://doi.org/10.1186/s40623-023-01885-6

Zhu C, Cotton F, Kawase H, Haendel A, Pilz M, Nakano K (2022) How well can we predict earthquake site response so far? Site-specific approaches. Earthq Spectra 38:2. https://doi.org/10.1177/87552930211060859

Publisher's Note